



An Automatic Surgical Decision Support Method for Radial Metaphyseal Fractures in X-Ray

Avigail Suna¹ MSc, Amit Davidson² MD, Prof. Yoram Weil² MD,
Prof. Leo Joskowicz^{1*} PhD.

¹ School of Computer Science and Engineering, The Hebrew University of Jerusalem, ISRAEL.

² Department of Orthopaedics, Hadassah University Medical Center, Jerusalem, ISRAEL
josko@cs.huji.ac.il, hoderk@cs.man.ac.uk

1 Purpose

Distal Radius Fractures (DRFs) are the most common type of fracture with a high incidence rate, accounting for 17.5% of all adult fractures. The established clinical workflow for patients with a suspicion of DRF calls for the acquisition of two radiographic X-ray images (radiographs) of the wrist in anteroposterior (AP) and lateral (LAT) views [1]. Radiographic parameters (RPs), which are linear angle and distance measurements derived from the AP and LAT radiographs, have been shown to provide objective support for effective decision making in determining clinical treatment of distal radius fractures (DRFs) [2]. Recently, we showed that providing computed RPs to orthopedic surgeons may improve the consistency of the radiographic judgment and influence their clinical decision for the treatment of DRFs [3]. However, calculating the RPs manually from radiographs requires experience, is time consuming, and is subject to observer variability.

This paper presents a novel deep learning automatic method for computing the six anatomical RPs associated with DRFs in AP and LAT forearm radiographs.

2 Methods

The method consists of a pipeline with three main steps: 1) segmentation of the distal (upper part) radius and ulna bones with six 2D Dynamic U-Net deep learning models; 2) landmark points detection and distal radius axis computation from the segmentations with geometric methods; 3) RP computation from the landmarks and generation of a quantitative DRF report and composite AP and LAT radiograph images. The pipeline is designed to handle a very wide variety of forearm radiographs from different sources, hand orientations, and with and without cast.

The first step consists of: 1) bounding box detection; 2) forearm segmentation; 3) radius segmentation; 4) distal bone segmentation. The first two steps normalize the radiographs and reduce their variability. The last two steps perform the actual segmentation. They are produced with three 2D Dynamic U-Net models [4] in which the encoder has pre-trained ResNet18 blocks and the decoder has ICNR blocks. The Focal, Dice, and Dice Contour Losses are used together with training time augmentations, e.g., rotation, flipping, homogeneous scaling, brightness scaling, contrast adjustment. The outputs are the segmentations of the radius and ulna segmentations in AP and the radius in LAT.

In the second step, the landmark points are computed from the bone segmentations. The AP landmarks lie on the distal radius and distal ulna contours. The LAT landmarks lie on the distal radius contour. For both, the input radiographs are aligned left-handed and rotated to align the radius axis with the y axis. Four landmarks are extracted from the AP radiograph: Styloid Tip (ST), Ulna Border of Radius (UBR), Radial Metaphyseal Border (RMB), Ulnar Height (UH); three are extracted from the LAT radiograph: Volar Joint Border (VJB), Dorsal Joint (DJ), Dorsal Metaphyseal (DM).

In the third step, the RPs are computed from the landmark points by creating lines from the landmark pairs and computing the angles and distances following the guidelines in [2] The output is a list of measurements and their reference nominal values.

3 Results

The pipeline was evaluated on a dataset of 90 AP and 93 LAT radiographs. Ground truth distal radius and ulna segmentations and RP landmarks were manually obtained by an expert clinician. Our method achieves an accuracy of 94% and 86% on the AP and LAT RPs, within the observer variability and an RP measurement difference of $1.4 \pm 1.2^\circ$ for the radial angle, $0.5 \pm 0.6\text{mm}$ for the radial length, $0.9 \pm 0.7\text{mm}$ for the radial shift, $0.7 \pm 0.5\text{mm}$ for the ulnar variance, $2.9 \pm 3.3^\circ$ for the palmar tilt and $1.2 \pm 1.0\text{mm}$ for the dorsal shift. Fig. 2 shows two examples.

4 Conclusion

Our method for computing anatomical RPs associated with DRFs in AP and LAT forearm radiographs is unique in that it is automatic, that it accurately and robustly computes the RPs for a wide variety of forearm radiographs from different sources, with various orientations, with and without cast. Unlike other deep learning methods [4], it requires a small (~100) dataset of manual annotations, and generates a quantitative DRF report that includes the RP values, their normal ranges, and the two radiographs with the detected landmarks from which the RPs were computed overlaid on them. It achieves wide coverage and robustness with multiple intensity normalization, forearm ROI detection and bone segmentation refinement stages. Our experimental studies show that our pipeline achieves a very high accuracy, within the observer variability, as reported for other tasks [5].

Automated RP computation on clinical forearm radiographs may improve clinical decision making and increase the consistency and adherence to guidelines by providing accurate and reliable measurements for fracture severity.

References

1. Kamal RN, Shapiro LM. American Academy of Orthopaedic Surgeons. American Society for Surgery of the Hand Clinical Practice Guideline summary management of distal radius fractures. *J. American Academy of Orthopaedic Surgeons* 30(4):e480ee486, 2020.
2. Wilcke MK, Abbaszadegan H, Adolphson PY. Patient-perceived outcome after displaced distal radius fractures: a comparison between radiological parameters, objective physical variables and the DASH score. *J. Hand Therapy* 20(4):290–299, 2007.
3. Davidson A, Suna A, Joskowicz L, Weil Y. Computer generated radiographic measurements of distal radius fractures – does it help with decision making? *J. Hand Surgery*, 2022.
4. Payer C, Štern D, Bischof H, Urschler M. Integrating spatial configuration into heatmap regression based CNNs for landmark localization. *Medical Image Analysis* 54:207–219, 2019.
5. Blüthgen C, Becker AS, de Martini IV, Meier A, Martini K, Frauenfelder T. Detection and localization of distal radius fractures: deep learning system versus radiologists, *European J. Radiology* 126:108925, 2020.

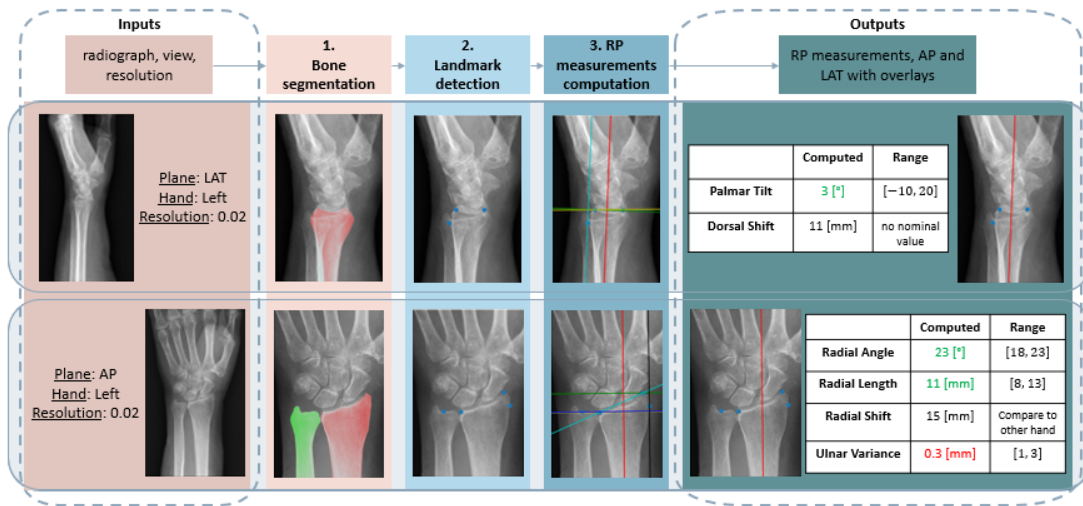


Figure 1: Block diagram of the pipeline for the automatic computation of the DRF report. The inputs are the two radiographs, their view label (AP/LAT), their hand label (Left/Right) and the pixel resolution (mm). The output is a DRF report with the computed RP values and their normal ranges and radiographs with the detected landmarks and axes overlaid on them. The main steps are: 1) Bone segmentation (distal radius and ulna in AP, distal radius in LAT); 2) Landmark extraction from the bone segmentations, and; 3) RP measurements computation.

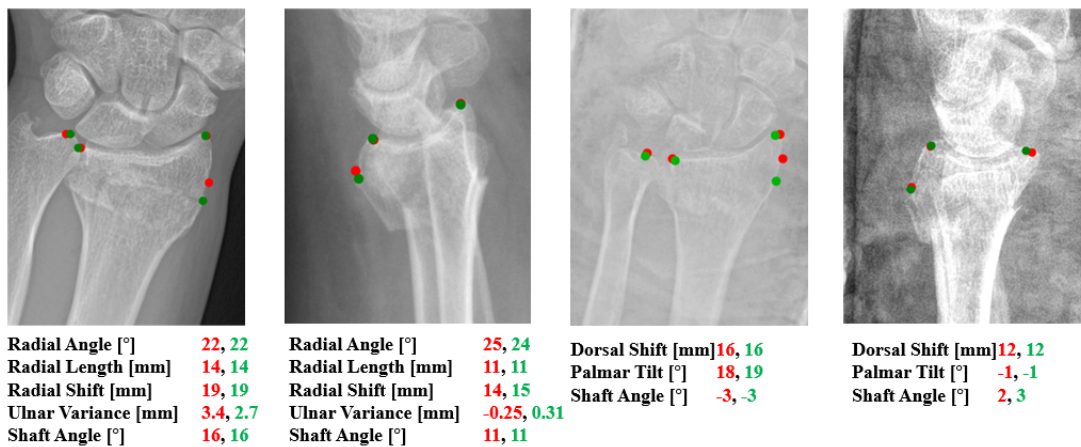


Fig. 2: Examples of the ground truth (green) and computed (red) landmarks and RP measurements in: a) AP radiograph, no cast; b) LAT radiograph, no cast; c) AP radiograph, with cast; d) LAT radiograph, with cast.